Pouring flow pattern visualization using digital twin technology in evaluation system of manual pouring work

Reo Fuse[1], Yoshiyuki Noda[2], Seishi Tsuyama[3], and Kazuya Asano[4]

1. Course of Mechanical Engineering, Integrated Graduate School of Medicine, Engineering, and Agricultural Sciences, University of Yamanashi, 4-3-11 Takeda, Kofu, 400-8511, Japan
2. Department of Mechanical Engineering, Graduate Faculty of Interdisciplinary Research, University of Yamanashi, 4-3-11 Takeda, Kofu, 400-8511, Japan
3. Isobe Iron Works Co., Ltd., Kitakyushu, Fukuoka, Japan
4. Isobe Iron Works Co., Ltd., Kitakyushu, Fukuoka, Japan

*Corresponding address: e-mail: g24tm027@yamanashi.ac.jp

Abstract: This study contributes to a sophisticated evaluation system of a pouring work by manual operation in the foundry industry. The manual pouring work has been used in the foundries with high-mix low-volume production. In the manual pouring work, the skilled workers are needed for producing the high quality casting products. However, it is difficult to inherit the skills because the pouring work has not been evaluated explicitly. Therefore, in this study, we propose the pouring flow pattern visualization system based on the digital twin environment of the manual pouring work. In the proposed approach, the model parameters in the mathematical pouring process model can be extracted systematically by scanning the practical ladle using the three dimensional (3D) scanner and extracting the model parameters using the application programming interface (API) function in the 3D-computer aided design (CAD). The ladle’ s motion can be measured by the inertia measurement unit (IMU) sensor, and the outflow molten metal from the ladle can be measured by the crane scale. The pouring flow rate can be estimated by simulating the pouring process model with the measurement data. Furthermore, the estimation results of the flow rate are visualized clearly by applying the Hampel filter and the finite-impulse-response type zero-phase filter. The efficacy of the proposed approach is verified by the experiments in the practical pouring works with the manual operation.

Keywords: manual pouring; flow rate estimation; digital twin; 3D scanning; CAD-based modeling; skill evaluation; noise reduction;

1 Introduction

In the casting industry, there is a pouring process in which high-temperature molten metal is poured into a mold from ladle. This process creates a dangerous environment for the workers because of involving the high-temperature molten metal and dust exposure [1,2]. In recent years, automatic pouring machines have been developed and applied in the foundries with mass production. However, it is difficult to apply the pouring machines in the foundries with high-mix low-volume production. In these foundries with high-mix low-volume production, the pouring pattern has to be changed corresponding to a wide variety of casting products, and the molten metal is poured by the manual operation of skilled workers.

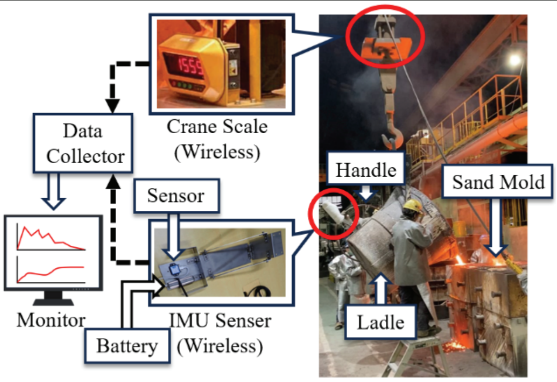

Fig.1: Measurement System for Pouring Work by Manual Operation

Therefore, the inheritance of knowledge and skill in the pouring work is the key to continuing performance of the foundries. Currently, on-the-job-training has been applied to acquire the skills required in the practical pouring work. However, the pouring work by a novice worker increases risk of the accident. Moreover, it is difficult to acquire the skill in the on-the-job-training without a quantitative assessment to the pouring work. In previous studies on the automatic pouring machines, the mathematical model with nonlinearity of the pouring process based on the liquid's volume balance in the ladle and Bernoulli's theorem has been derived in [3-5]. The real-time pouring flow rate estimation and the feedback control based on the mathematical model have been proposed for realizing the high precision automatic pouring machine [6,7]. Furthermore, the training simulators for acquiring the skill of manual pouring work have been developed using the virtual reality technologies and the game design [8,9]. However, few studies have been reported on quantitative evaluation of the actual pouring work by the manual operation. The quality of casting products is influenced by the pouring flow pattern in the manual pouring work.

In this study, we propose the pouring flow pattern visualization approach for evaluating quantitatively the pouring work by the manual operation. In this approach, the pouring flow rate as the flow pattern can be estimated by the digital twin technology with the mathematical model of pouring process. For designing the pouring process model, inner geometry of the ladle in practical use can be measured by a handy three dimensional (3D) scanner, and the model parameters are extracted from the measured inner geometry of the ladle using the application programming interface (API) function in 3D-computer aided design (CAD). Posture angle of the ladle and weight of outflow molten metal from the ladle while pouring the molten metal can be measured by an inertia measurement unit (IMU) sensor and a crane scale, respectively. The flow rate can be estimated by inputting the measurement data to the pouring process model. In order to improve the quantitative visualization of the estimation result, the Hampel filter [10] and the zero-phase filter are applied. The efficacy of the proposed approach is verified by implementing it to the actual pouring work by the manual operation.

2 Measurement system of manual pouring work

In this study, we develop the measurement system to quantitatively measure the weight of outflow molten metal and the tilting behavior of the ladle during the pouring work. It enables to apply in an actual manufacturing environment during the operator's pouring process using molten metal. The weight of outflow molten metal from the ladle and the tilting angle of the ladle on the pouring work can be measured by the crane scale and the IMU sensor as shown in Fig.1, respectively. The crane scale is located between the crane hook and the hoisting attachment of the ladle. The IMU sensor is attached to the ladle. Both sensors are connected wirelessly to the data collector. The pouring flow rate can be estimated using the measurement data in the data collector and visualized graphically in the monitor.

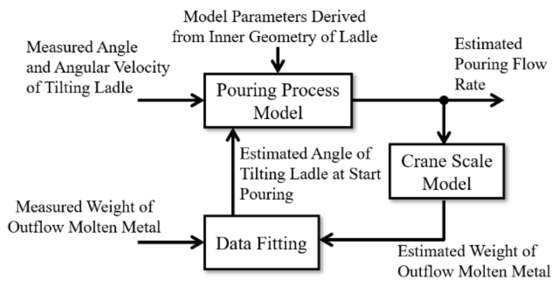

Fig. 2: Pouring Flow Rate Estimation System

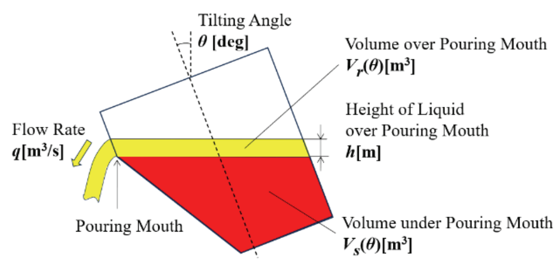

Fig. 3: Schematic Overview of Pouring Process

3 Pouring flow pattern visualization by digital twin technology

In the pouring flow pattern visualization, the pouring flow rate estimation system can be constructed flow rate estimation system can be constructed as shown in Fig.2. The pouring flow rate can be estimated by fitting the behavior of pouring process model to the actual measurement data. The pouring process model, the crane scale model, the model parameters derivation from the inner geometry of ladle and the data fitting are detailed in the next subsection.

3.1 Pouring Process Model

In the pouring work by the manual operation, the molten metal is poured from the ladle by rotating the handle attached to the side of the ladle by an operator. Fig.3 shows the process which the molten metal is flowing out of the ladle. The ladle is tilted by the operator's handle manipulation. Using the IMU sensor attached to the ladle, the tilting angular velocity ω [deg/s] and the tilting angle θ [deg] can be measured. The relationship between the ladle' s angular velocity and tilting angle is given as

$$\frac{d\theta(t)}{dt} = \omega. \qquad (1)$$

In Fig.3, the liquid's volume under the pouring mouth is V_s [m^3], the liquid's volume over the pouring mouth is V_r [m^3], the liquid's height over the pouring mouth is h [m], and the outflow liquid's flow rate from the ladle is q [m^3/s]. The volume balance equation of the liquid over the pouring mouth can be represented as

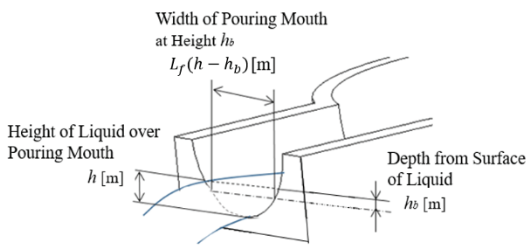

Fig. 4: Parameters on Pouring Mouth

$$\frac{dV_r(t)}{dt} = -q(t) - \frac{dV_s(t)}{dt}. \qquad (2)$$

The liquid volumes V_r and V_s can be obtained from the ladle shape. The volume V_s depends on the ladle's tilting angle θ. Thus, its time derivative can be represented as

$$\frac{dV_s(t)}{dt} = \frac{\partial V_s(\theta)}{\partial \theta}\frac{d\theta(t)}{dt} = \frac{\partial V_s(\theta)}{\partial \theta}\omega(t). \qquad (3)$$

The volume V_r depends on the tilting angle θ and the liquid height h. Thus, the time derivative of V_r can be represented as

$$\frac{dV_r(t)}{dt} = \frac{\partial V_r(\theta,h)}{\partial \theta}\omega(t) + \frac{\partial V_r(\theta,h)}{\partial h}\frac{dh(t)}{dt}. \qquad (4)$$

By substituting Eqs.(3) and (4) into Eq.(2), the behavior of liquid' s height on the pouring mouth can be represented as

$$\frac{dh(t)}{dt} = -\frac{q(t)}{\frac{\partial V_r(\theta,h)}{\partial h}} - \frac{\frac{\partial V_r(\theta,h)}{\partial \theta} + \frac{\partial V_s(\theta)}{\partial \theta}}{\frac{\partial V_r(\theta,h)}{\partial h}}\omega(t), \qquad (5)$$
$$(\theta \geq \theta_s, h \geq 0)$$

where θ_s is the ladle' s angle at starting outflow liquid. The flow rate of the outflow liquid from the ladle depends on the geometry of pouring mouth and the liquid height on the pouring mouth. The geometry of pouring mouth is shown in Fig.4. In Fig.4, the liquid depth from the liquid surface is h_b [m], and the width of the pouring mouth at the liquid height $h - h_b$ is

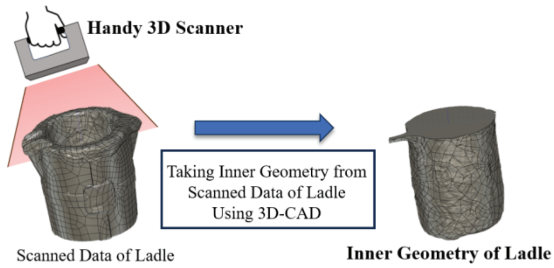

Fig. 5: Method for Taking Inner Geometry of Ladle Using 3D-Scanner and 3D-CAD

$L_f(h - h_b)$ [m]. The relation between the liquid height and the flow rate of the outflow liquid from the ladle can be derived using Bernoulli's theorem as

$$q(h(t)) = c\int_0^{h(t)} L_f(h(t) - h_b)\sqrt{2gh_b}\,dh_b, \qquad (6)$$
$$(0 \leq c \leq 1)$$

where g is a gravitational acceleration, and c is a flow rate coefficient. The pouring process model consists of Eqs. (5) and (6). In this model, the model parameters related to the geometry of the ladle can be obtained by the geometry measurement using 3D-scanner. And, the flow rate coefficient and the tilting angle of the ladle at starting outflow liquid can be obtained by fitting the simulation result of the outflow liquid' s weight to the measurement data of that.

3.2 Crane Scale Model

The relationship between the outflow liquid' s weight W [kg] from the ladle and the flow rate q is shown as

$$\frac{dW(t)}{dt} = \rho q(t), \qquad (7)$$

where ρ [kg/m^3] is the liquid density. The weight of outflow liquid from the ladle can be measured by the crane scale attached between the crane hook and the attachment for hoisting ladle. The dynamics of the crane scale can be represented as the first-order lag system as follows:

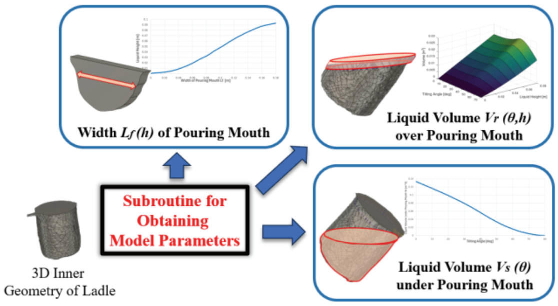

Fig. 6: Model Parameters Extraction System by API Function in 3D-CAD

$$\frac{dW_L(t)}{dt} = -\frac{1}{T_L}W_L(t) + \frac{1}{T_L}W(t), \qquad (8)$$

where W_L [kg] is the outflow liquid's weight measured by the crane scale, and T_L [s] is the time constant of the crane scale.

3.3 Model Parameters Derivation from Geometry of Ladle

For designing the proposed flowrate estimation system, it is required to obtain the model parameters from the ladle shape: (i) the liquid volume V_r (θ, h) over the pouring mouth, (ii) the liquid volume $Vs(\theta)$ under the pouring mouth, and (iii) the pouring mouth's width L_f (h). However, it is difficult to derive analytically the model parameters because the practical ladle has a complicated shape and multiformity depending on casting environment. In order to apply the proposed flow rate estimation system to the practical use in foundry, we need to obtain quickly and systematically Fig.6. Model Parameters Extraction System by API Function in 3D-CAD these model parameters from the shape of the practical ladle. Therefore, we developed the model parameters extraction system which the model parameters in Eqs. (5) and (6) are extracted from the geometry data of the practical ladle. The practical ladle can be scanned by a handy 3D scanner for obtaining the geometry data of the ladle as shown in Fig.5. The geometry data obtained by scanning the ladle is fed directly into a 3D-CAD, and the inner geometry of the ladle is taken out of the scanned data in the 3D-CAD. The model parameters V_s, V_r and L_f subsequently can be extracted from the inner geometry data of the ladle as shown in Fig.6. We have used the API function in the 3D-CAD for automatically extracting the model parameters. In the extraction system, the sampling intervals of the liquid height h and the tilting angle θ are Δh = 0.001 m and $\Delta\theta$ = 1.0 deg, respectively. Figs.7 and 8 show respectively the liquid volumes V_r over the pouring mouth and V_s under the pouring mouth derived by the model parameters extraction system developed in this study. And, Fig.9 also shows the width L_f of the pouring mouth. As shown in Figs. 7-9, we can obtain the high-definition model parameters related to the practical ladle by the developed extraction system.

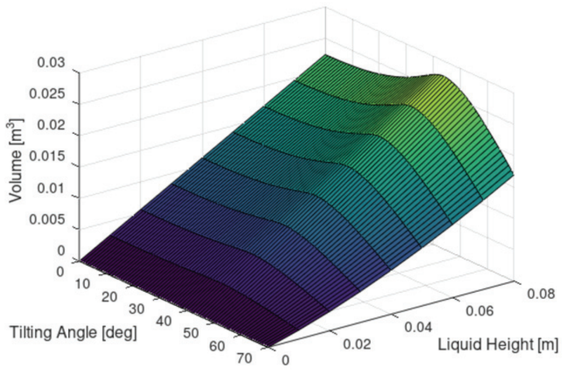

Fig. 7: Liquid Volume $V_r(\theta, h)$ over Pouring Mouth

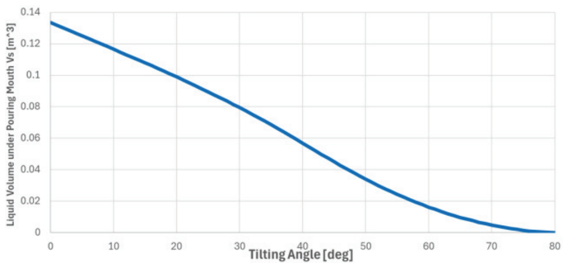

Fig. 8: Liquid Volume $V_s(\theta)$ under Pouring Mouth

In the pouring process model, the differential forms of the model parameters V_r and V_s are used. Therefore, these are approximated as

$$\frac{\partial V_r(\theta_i, h_j)}{\partial \theta} \approx \frac{V_r(\theta_{i+1}, h_j) - V_r(\theta_i, h_j)}{\Delta\theta},$$

$$\frac{\partial V_r(\theta_i, h_j)}{\partial h} \approx \frac{V_r(\theta_i, h_{j+1}) - V_r(\theta_i, h_j)}{\Delta h},$$

$$\frac{\partial V_r(\theta_i, h_j)}{\partial \theta} \approx \frac{V_r(\theta_{i+1}) - V_r(\theta_i)}{\Delta\theta},$$

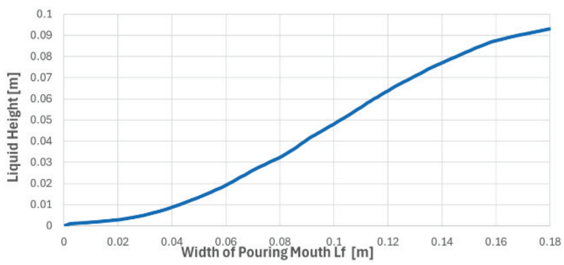

Fig. 9: Width Lf (h) of Pouring Mouth

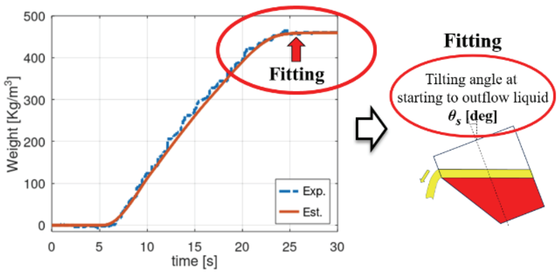

Fig. 10: Measurement and Simulation Results of Weight of Outflow Liquid from Ladle after Identification of Tilting Angle θs at Starting Outflow Liquid and Flow Rate Coefficient c

where i and j are the index numbers of the vectors θ and h, respectively. The pouring process model's accuracy is increased with a decrease in the sampling intervals $\Delta\theta$ and Δh.

3.4 Data Fitting Simulation to Measurement data

In the model parameters, the tilting angle θ_s of the ladle at starting outflow liquid and the flow rate coefficient c are identified by fitting the weight W_L of the outflow liquid from the ladle simulated by the pouring process model to that measured by the crane scale. The gross weight of the outflow liquid can be influenced largely by the tilting angle θ_s at starting outflow liquid. Therefore, the tilting angle θ_s at starting outflow liquid was identified by fitting the gross weight of the outflow liquid in the simulation to that in the measurement data. The flow rate coefficient c was identified by minimizing the integral square error between the timeseries weights of the outflow liquid in the simulation and the measurement data. Fig.10 shows the simulation result of outflow liquid weight W_L after the data fitting and the measurement data by the crane scale.

In Fig.10, the red line is the simulation result and the

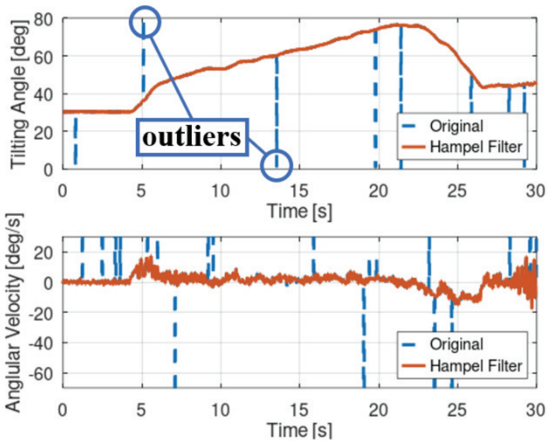

Fig. 11: Outliers Appeared in Measurement Data by IMU Sensor and Results of Outliers Removal Using Hampel Filter

blue line is the measurement data. The simulation by the pouring process model can be represented adequately to the actual pouring work. In this study, the tilting angle θ_s and the flow rate coefficient c were identified as $\theta_s = 32.7$ deg and $c = 0.89$, respectively.

3.5 Outliers and Noise Reduction by Filters

In the pouring flow rate estimation system, the pouring work can be simulated by applying the measurement data in the manual pouring work, the model parameters derived from the geometry of the ladle to the pouring process model. However, the data of the ladle's tilting angle and the angular velocity measured by the IMU sensor contain a significant amount of outliers and noise. The accuracy of the flow rate estimation can be degraded by the outliers and the noise. Moreover, it is required to visualize clearly the result of the pouring flow rate for evaluating the manual pouring work. Therefore, we propose the outlier and noise reduction approach using the signal processing. In this study, the outliers can be removed by the Hampel filter, and the noise can be suppressed by the finite-impulse-response type zero-phase filter (FIR-ZPF). The design methods for these filters are detailed in the next subsection.

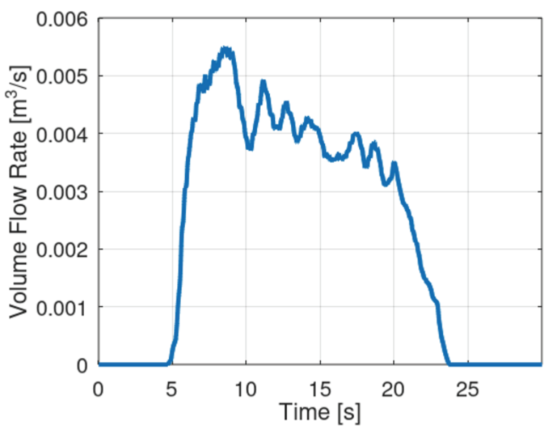

Fig. 12: Estimation Results of Pouring Flow Rate

3.5.1 Outliers Removal Using Hampel Filter

The data gaps can be occurred in the detection of the tilting angle and the angular velocity due to the wireless communication between the IMU sensor and the data collector, and are appeared as the outliers as shown in Fig.11. The simulation using the pouring process model can be failed by the outliers.

In order to remove the outliers, we apply the Hampel filter to the measurement data before estimating the pouring flow rate. The Hampel filter is a robust outlier detection technique that uses a moving window to compare each data point with the median of its surrounding values. By using the median and the median absolute deviation instead of the mean and standard deviation, the filter enables to be insensitive to the extreme values. The orange lines in Fig.11 show the results the outliers were removed by the Hampel filter. The flow rate estimation can be performed using the tilting angle and the angular velocity with removing the outliers as shown in Fig.12.

3.5.2 Design of FIR-ZPF

In order to remove the outliers, we apply the Hampel filter to the measurement data before estimating the pouring flow rate. In the evaluation of the manual pouring work, it is required to visualize clearly the estimated pouring flow rate. Therefore, the visualization of the pouring flow rate can be improved by reducing the noise in the measurement data by IMU sensor. A low-pass filter (LPF) is generally applied for reducing the noise. However, the estimated pouring flow rate can be distorted by an ordinary LPF with a phase lag. Therefore, we apply the FIR-ZPF for the noise reduction without the phase lag. The FIR-ZPF cannot be used for the real-time processing. On the other hand, in the proposed system, the pouring flow rate can be estimated with a batch processing, and the estimation result is shown in the monitor after the batch processing. The FIR-ZPF can be used for the noise reduction by the batch processing. The FIR-ZPF consists of the sinc function and hann window in this study. The sinc function is represented as

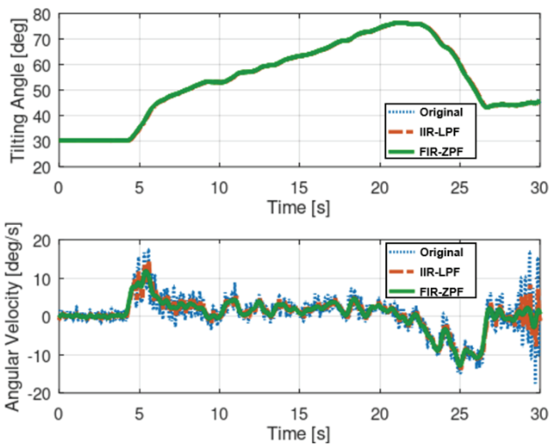

Fig. 13: Noise Reduction in Measurement Data using Filters

$$h(t) = \frac{\omega_c}{\pi} \cdot \mathrm{sinc}\left(\frac{\omega_c t}{\pi}\right). \qquad (9)$$

where ω_c is the cut-off angular frequency. For suppressing the ripples in the frequency domain, the following hann window is also applied:

$$w(t) = 0.5\left(1 + \cos\left(\frac{2\pi t}{T}\right)\right), \qquad (10)$$
$$\left(-\frac{T}{2} \le t \le \frac{T}{2}\right).$$

where T is the total window length in time. The final filtered output signal $y(t)$ is obtained by convolving the input signal $x(t)$ with the symmetric windowed impulse response $h(t)w(t)$. The following symmetric convolution ensures a zero-phase response:

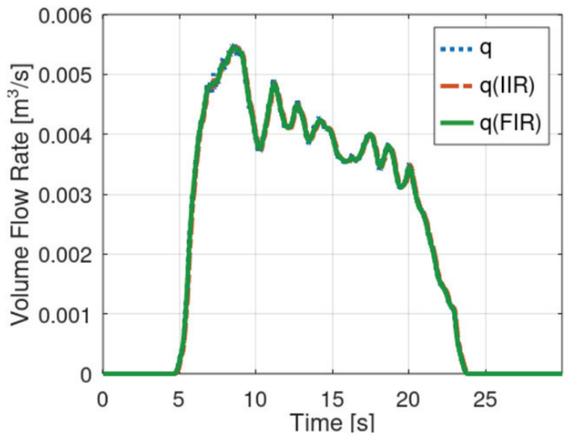

Fig. 14: Pouring flow rate estimation after noise reduction

$$y(t) = \int_{-T/2}^{T/2} h(\tau)w(\tau) \cdot x(t-\tau)\, d\tau. \qquad (11)$$

By applying the windowed and normalized impulse response in this manner, it is possible to reduce high-frequency noise while preserving the original waveform shape without the phase distortion.

4 Experimental Verification

The efficacy of the noise reduction using the FIR-ZPF is verified by the proposed flow rate estimation with applying the FIR-ZPF to the measurement data by IMU sensor. In this study, the cutoff frequency is set to f_c = 2 Hz, and the corresponding angular frequency is defined as $\omega_c = 2\pi f_c$. The cutoff frequency represents the boundary at which the filter begins to attenuate the frequency components of the input signal, effectively suppressing higher frequency components beyond this threshold. According to previous studies, the upper limit of vibration frequency that a human operator can manually control is approximately 1.4 Hz. Based on this knowledge, the cutoff frequency is set to 2 Hz in this study to suppress the noise components exceeding 1.4 Hz. The window width of the FIR-ZPF is set to T = 1.0 [s]. As the comparative verification, we also apply the infinite-impulse- response type low-pass filter (IIR-LPF) to reduce the noise in the measurement data by the IMU sensor. In this filter, the cut-off frequency is same as the FIR-ZPF. Both filters are applied to the measured tilting angle and angular velocity data. The resulting filtered signals are shown in Fig.13. Additionally, the estimated pouring flow rates q [m^3/s], which are obtained using the filtered signals, are shown in Fig.14.

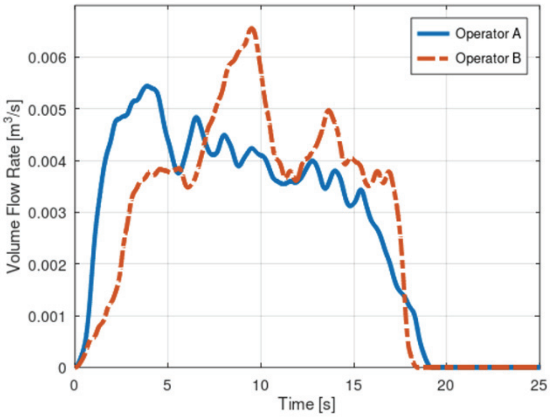

Fig. 15. Comparison of Pouring Behavior between Operators with Applying Zero-Phase Filter

Table 1. Composition of Flow Filtering Methods

Method	ISE[(m^3/s)^2·s]	TV[m^3/s]
IIR-LPF	2.0348×10^{-8}	3.9240×10^{-3}
FIR-ZPF	1.0703×10^{-8}	2.8080×10^{-8}

The performances of the both filters was evaluated using two quantitative metrics. The first evaluation metric is the integral of squared error (ISE), which measures the discrepancy between the filtered estimated flow rate and the estimated flow rate without the filters. ISE is defined as

$$\text{ISE} = \sum_{i=1}^{N} (\hat{q}_i - q_i)^2 \Delta t. \tag{12}$$

where $\hat{q}_i$ denotes the estimated flow rate after applying the filter, q_i represents the estimated flow rate without filtering, and Δt is the sampling interval. A lower ISE indicates that the filtered signal better retains the original characteristics of the baseline data. The second metric is the Total Variation (TV), which evaluates the degree of fluctuation in the estimated flow rate. TV is a measure of the smoothness of the signal and is calculated as

$$\text{TV} = \sum_{i=1}^{N-1} |q_{i+1} - q_i|, \tag{13}$$

where, q_i denotes the estimated flow rate at time step i. A smaller TV value implies a smoother signal with the adequate noise reduction The results are presented in Table I. As can be seen from the table, both the ISE and TV values for the FIR-ZPF are lower than those for the IIR-LPF. This result indicates that the FIR-ZPF achieves smoother variations in the estimated flow rate while preserving the original signal characteristics. Therefore, it can be concluded that the application of the FIR-ZPF is more effective for noise reduction in pouring flow rate estimation compared to the IIR-LPF.

3.3 Comparison of Pouring Behavior between Operationas

By applying the proposed pouring flow rate estimation based on the digital twin technology with the FIR-ZPF, we can visualize differences in pouring behavior among operators. Fig.15 shows a comparison between a skilled operator (Operator A) and a novice operator (Operator B). As seen from Fig.15, operator A achieves a quicker rise in flow rate and maintains a more stable pouring volume throughout the task compared to Operator B. These results demonstrate that digital twin-based flow rate estimation is a highly effective approach for quantitatively evaluating the pouring work.

4 Conclusions

We proposed the pouring flow pattern visualization system of the pouring work with the manual handling in the iron foundries with high-mix low-volume production. The significance of this work lies in two main contributions. First, we developed a simple and efficient approach to derive geometric parameters required for simulation by utilizing the API functions of 3D-CAD software. This enables automatic extraction of complex ladle parameters that are otherwise difficult to compute manually. Second, we applied the FIR-ZPF for the noise reduction, which effectively smooths the estimated signal without introducing phase lag, while preserving the original characteristics of the measured data. This allows for more accurate identification of the true pouring behavior. The proposed method provides a promising approach for quantitatively evaluating pouring skills and serves as a useful foundation for comparing the performance of skilled and novice operators. These results demonstrate that the proposed system can contribute to the development of more effective skill assessment and knowledge transfer techniques in the casting industry.

Conflicts of interest:

The authors declare that they have no known competing financial interests or personal relationships that could have appeared to influence the work reported in this paper.

References

[1] L. Li, C. Wang, and H. Wu, "Research on kinematics and pouring law of a mobile heavy load pouring robot," Mathematical Problems in Engineering, vol. 2018, Art. no. 8790575, 2018, doi:10.1155/2018/8790575.

[2] K. Yano and K. Terashima, "Supervisory control of automatic pouring machine," Control Engineering Practice, vol. 18, pp. 230–241, 2010.

[3] Y. Noda and T. Nishida, "Precision analysis of automatic pouring machines for the casting industry," International Journal of Automation Technology, vol.2, pp. 241–246, 2008.

[4] Y. Noda and K. Terashima, "Modeling and feedforward flow rate control of automatic pouring system with real ladle," Journal of Robotics and Mechatronics, vol. 19, pp. 205–211, 2007.

[5] N. Kabasawa and Y. Noda, "Model-based flow rate control with online model parameters identification in automatic pouring machine," Robotics, vol. 10, no. 1, 2021, doi: 10.3390/robotics10010039.

[6] Y. Noda and Y. Sueki, "Implementation and experimental verification of flow rate control based on differential flatness in a tilting-ladle-type automatic pouring machine," Applied Sciences, vol.9, no. 10, Art. no. 1978, 2019, doi: 10.3390/app9101978.

[7] Y. Sueki and Y. Noda, "Experimental verification of real-time flow-rate estimations in a tilting-ladle-type automatic pouring machine," Applied Sciences, vol. 11, no. 15, Art. no. 6701, 2021, doi: 10.3390/app11156701.

[8] T. Miura and Y. Noda, "Development of pouring work training simulator with indicating operation score for efficient skill acquisition," in Proceedings of the 2025 IEEE/SICE International Symposium on System Integration (SII), 2025, pp. 924–929.

[9] T. Miura and Y. Noda, "Development of training simulator with graphs of operational status for efficient acquisition of pouring skill in casting industry," in Proceedings of the 2024 International Symposium on Flexible Automation (ISFA), 2024, pp. 141225(1)–141225(5).

[10] F. R. Hampel, "The influence curve and its role in robust estimation," Journal of the American Statistical Association, 69, 1974, pp.382–393.

[11] Y. Noda and D. Suzuki, "Operational assistance system for vibration suppression and precise positioning in manual guided transfer system," in Proceedings of the 2015 IEEE International Conference on Systems, Man, and Cybernetics (SMC), 2015, pp. 1244–1249.